

PHYSICAL REVIEW B

CONDENSED MATTER

THIRD SERIES, VOLUME 37, NUMBER 5

15 FEBRUARY 1988-I

Al $L_{2,3}$ and Mg double-ionization emission spectra of dilute Al in Mg alloys

C. H. Zhang, K. -L. Tsang, and T. A. Callcott*
University of Tennessee, Knoxville, Tennessee 37996

D. L. Ederer
National Bureau of Standards, Gaithersburg, Maryland 20899

E. T. Arakawa
Oak Ridge National Laboratory, Oak Ridge, Tennessee 37830
(Received 11 June 1987)

The Al $L_{2,3}$ spectrum for dilute alloys of Al in Mg, and the Mg L satellite spectrum produced by transitions in atoms with doubly ionized $2p$ core levels have been measured. The two spectra contain similar features associated with screening of the extra core hole, but are otherwise dissimilar, which suggests that the equivalent-core approximation is not valid. The threshold peak is broadened in both spectra. The Al-impurity spectrum is found to be about 1 eV wider than that of the Mg host. The L_3 - L_1 intercore transition in doubly ionized Mg is observed. Finally, a second, weak, high-energy satellite of Mg is observed that may be produced by transitions from the 1S_0 state of the doubly ionized core levels. These results provide important new data for comparison with theories of the electronic states of impurity atoms in metals.

INTRODUCTION

Soft-x-ray emission (SXE) spectroscopy provides a detailed map of the filled electronic states of alloys and provides a rigorous check of alloy theories, particularly those treating effects occurring in the region near the constituent atoms, where theories based on average potentials are least reliable. In this paper, we present SXE emission spectra from dilute Al in Mg alloys and from doubly core-ionized ($2p^2$) Mg atoms, both of which can be viewed as isolated impurity atoms with a single excess charge in a Mg host lattice. The data provide a clear measure of the changes in local density of states which result from static screening of the excess charge.

SXE spectra from alloys are produced by radiative transitions from conduction-band states, characteristic of the solid, to empty atomic core states of one constituent of the alloy. The empty core states may be produced by either energetic electrons or photons. Since the final states are localized on a single atom, and the transitions obey the $\Delta l = \pm 1$ angular momentum selection rule, the SXE spectra provide a measure of the partial density of states (PDOS) in a region localized near a selected constituent of the alloy. In these studies of Al-Mg alloys, the Al(Mg) $L_{2,3}$ spectrum results from transitions to the

$2p$ core state so that the spectrum provides a measure of the ($s+d$) PDOS in a region near the Al (Mg) atom. The Mg L satellite spectrum results from transitions to doubly ionized $2p$ core levels, and provides PDOS information for an atom with an excess core hole in the final state of the SXE transition.

Two-electron spectroscopies also provide information about the filled band states of the alloy. Photoemission spectroscopy (PES) provides a measure of the total DOS, without chemical, spatial, or angular momentum selectivity, but with greater sensitivity to surface states, and with the possibility of obtaining additional band-structure information from angle-resolved measurements. Auger electron spectroscopy (AES), in which both electrons originate in the band states (KVV or LVV spectra), is used for the chemical analysis of alloys, but DOS information is difficult to extract from the spectra which are produced by a convolution over the band states of both electrons.¹ Auger spectra, in which one electron makes an L to K intercore transition and a second is excited from the valence band (KL spectra), give information similar to SXE spectra. They provide DOS information for electron states localized on one chemical species, have some PDOS selectivity, and have an excess core hole in the final state of the transition.²

The KL_1V spectrum samples s and p states with approximately equal probability and thus provides a measure of the $(s+p)$ PDOS. Our SXE spectra from dilute Al in Mg alloys will be compared with previous SXE spectra on richer alloys^{3,4} and with the KL_1V Auger spectra.^{5,6}

Theories of the electronic states of alloys are intractable because of the mathematical difficulties imposed by disorder, though substantial progress has been made in recent years through the use of band-structure calculations employing the coherent-potential approximation.⁷⁻⁹ The study of dilute alloys is of particular interest because it permits comparison of experimental data on the dilute component with calculations made for single impurities in a host lattice. For metals, this problem has been discussed extensively using many-body theory,² static screening within the one-electron approximation,⁹⁻¹¹ and in terms of localized excitations.^{12,13} Al in Mg has additional interest because it is an example of the $Z+1$ problem in which an impurity (Al) with one excess core charge is placed in a host lattice (Mg) with $Z=2$ charges per ion. Several authors have previously published SXE studies on another $Z+1$ system, Mg in Li.^{14,15} In this paper we extend earlier studies of the Al-Mg system to the impurity limit, presenting data on 0.5-, 1-, and 2-at. % alloys.

An important assumption, usually called the final-state rule (FSR), is confirmed by both theory and experiment, and greatly simplifies the interpretation of SXE spectra derived from s and p electrons in light metals and semiconductors. Many-body theory indicates that the transition matrix elements may be calculated using the one-electron band states appropriate to the final-state configuration of the system.¹⁶⁻¹⁹ For SXE spectra, the final state of the transition is just the ground state of the system so that ordinary ground-state band-structure wave functions may be used. A large body of experimental SXE data also supports the FSR assumption. In simple metals, the spectra calculated using the FSR are modified by a prominent peak at the Fermi edge, usually referred to as the Mahan-*Nozières-de Dominicis* (MND) anomaly, associated with the dynamic screening of the core hole.^{20,21} The original theoretical derivations of the FSR and the threshold peak in metals from many-body theory involved detailed numerical calculations, but more recently both effects have been derived using the FSR approximation applied to orthogonalized final-state wave functions.¹⁹

Another assumption, the equivalent-core approximation (ECA), has sometimes been made in the interpretation of core spectra from various spectroscopies.² The ECA asserts that impurity ions carrying the same core charge should produce similar spectra. This idea is relevant in the present context because the Al-impurity spectrum, the Mg satellite spectrum, and the Mg KL_1V Auger spectra all provide a measure of an s -like PDOS for systems with a single excess charge in the final state, and thus are equivalent within the ECA. In this paper we compare our SXE spectra of dilute Al in Mg and our Mg satellite spectrum with the KL_1V Auger spectra published by others⁵ and show that the spectra have substantial differences. Thus the ECA does not provide a

useful common description for the three spectra.

Experiment^{4-6,14,15} and theory^{2,10,11} indicate that when a $Z+1$ impurity is placed in a nearly-free-electron metal, the bandwidth will be that of the host metal, but that there is a greatly enhanced s -PDOS near the bottom of the band associated with the static screening of the extra charge. We confirm this general characteristic for both the Al spectrum and the Mg satellite spectrum, but find substantial differences in the detailed forms of the spectra.

Several other characteristic features of SXE spectroscopy are relevant. Because radiative yields are low, emission spectra are weak, especially for the minor component of dilute alloys.²² The data presented here were taken with a new spectrometer whose greatly improved efficiency makes the measurement of 1% alloys and of satellite spectra routine.²³ The SXE spectra of metals have a low-energy tail, resulting from the presence of multielectron shakeup effects²⁴ which make it difficult to determine an accurate lower edge of the DOS. Additional tailing may result from plasmon satellites and clustering effects in alloys.^{25,26} Finally, the hole excitation and escape depths for SXE spectroscopy are usually such that it is primarily a bulk rather than a surface probe.

Though our new high-efficiency spectrometer allows us to acquire data for very weak spectra, great care is still required to extract accurate data on very dilute systems. Long integrations of weak spectra integrate not only the wanted signal but also the background, consisting of bremsstrahlung and scattered light, which must be subtracted from the spectra. Small errors in the calibration of the detector system, which have negligible effect on strong spectra, may appear as spurious structure in weak spectra. Self-absorption effects must be carefully considered. In the present case, the SXE spectra of Al lies in the absorption band of the host metal Mg. In the present system also, there is some overlap in the Al impurity spectra and the Mg satellite spectra, so that careful consideration has been given to separation of the two. Consequently, these subtraction procedures are described in the following section.

EXPERIMENTAL EQUIPMENT AND PROCEDURES

The SXE spectrometer used in these studies is a 5 m Rowland circle design with large toroidal gratings and a microchannel-plate enhanced charge-coupled-device (CCD) Si-diode array readout. Using a 600 line/mm grating and 100- μm slits, the theoretical resolution is better than 0.2 eV to photon energies of 90 eV. The instrument is used as a display-type instrument with about 10 Å of the spectrum being imaged by the CCD readout at each position of the detector. Spectra covering a wide range, such as those reported here, are assembled from spectral slices taken at 10-Å intervals. A detailed description of the instrument has been given elsewhere.²³

Measurements were made in an ion-pumped ultrahigh vacuum (UHV) chamber at a pressure of about 1×10^{-8} torr. Spectra were excited with a 0.2-mA beam of 2-kV

electrons imaged in a 1-mm spot on a sample placed 3 or 4 mm away from the entrance slit of the spectrometer.

For the measurements reported here, five samples (Al, Mg, and 0.5-, 1-, 2-at. % Al in Mg) were mounted and measured at the same time under identical conditions. The samples were prepared at the National Bureau of Standards (NBS) in the Metallurgy Division by melting together the components of the alloy, annealing for 24 h just below the melting point, and quenching in water. Wafers approximately 1 mm thick by 1 cm in diameter were sawn from the rod. Excitation and emission angles were 48° and 30° from the sample normal, respectively. The use of identical excitation conditions greatly facilitated the subtraction of background effects and the separation of the weak Al and Mg satellite spectra, as described below.

In the experiments reported here, the total spectrum from 155 to 325 Å was taken in 17 min in 17 segments. The partial spectrum in the impurity region from 165 to 195 Å was then recorded in three segments with six 5-min exposures of each segment (30 min per segment, 90 min total exposure). For each spectrum, a background consisting of detector and readout noise was subtracted before the raw data was multiplied by a transmission factor to account for nonlinearities in the detector system.

For these measurements, no correction has been made for the grating efficiency as a function of wavelength. As a result, quantitative comparisons of spectral intensities at widely separated wavelengths cannot be accurately made.

Spectra are recorded on a detector surface oriented tangentially (or within a few degrees of the tangent) to the Rowland circle.²³ When corrected for a "plate factor" similar to that required in the photographic recording of data,²⁷ the recorded spectra provide a direct measure of the wavelength-dependent spectral intensity $I(\lambda)$. These spectra may be converted to energy-dependent intensity spectra $I(E)$ by dividing the spectra by E^2 . All spectra in this paper are presented as a function of photon energy and have been divided by E^2 .

In Fig. 1, the spectrum of a 1 at. % Al in Mg alloy is plotted. The $L_{2,3}$ spectrum from the Mg host is visible below 50 eV. The inset shows the $L_{2,3}$ spectrum from 1 at. % Al and the Mg satellite spectrum after a 30 times longer integration of signal on the detector. The satellite spectrum extends to 64 eV and the Al impurity spectrum to about 73 eV. As we shall see below, there is some overlap between the Al spectrum and the Mg satellite spectrum so that they must be separated in order to get an accurate measurement of either.

For intense spectra which greatly exceed the background, backgrounds may often be subtracted using a straight-line fit to the baseline on either side of the spectrum. More careful procedures must be used in the present case, where structures comparable in magnitude to the background signal must be analyzed. Figure 2 shows the Al impurity spectra and the Mg L satellite for pure Mg and the three alloy samples with Al content of 0.5 at. %, 1 at. %, and 2 at. %. The spectra were taken under conditions of excitation and orientation that were

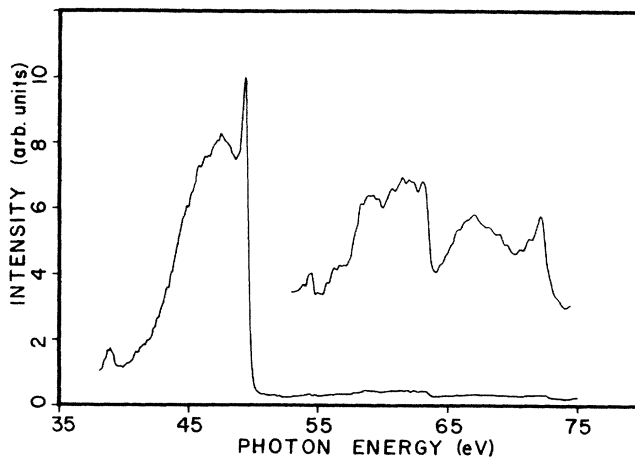


FIG. 1. The SXE spectrum of 1 at. % Al in Mg alloy. Major features are the Mg $L_{2,3}$ spectrum (42–50 eV), the Mg L double-ionization satellite spectrum (56–64 eV), and the Al $L_{2,3}$ impurity spectrum (64–73 eV).

as nearly identical as possible. The spectra are normalized to the peak height of the primary Mg spectrum to account for minor differences in sample position and excitation current. Assuming that the background contribution from the Mg in the dilute alloys was the same as for the pure Mg, the background and satellite spectrum of the pure Mg was subtracted from the alloy samples after appropriate normalization of the satellite to the primary spectra.

After subtraction, the spectra of 0.5 at. %, 1.0 at. %, and 2.0 at. % Al in Mg were obtained as shown in Fig. 3. The intensity increases linearly with impurity concentration as expected. A low-energy tail, which we believe to be real, that extends below the Mg satellite spectrum is observed. An increase in residual background with Al

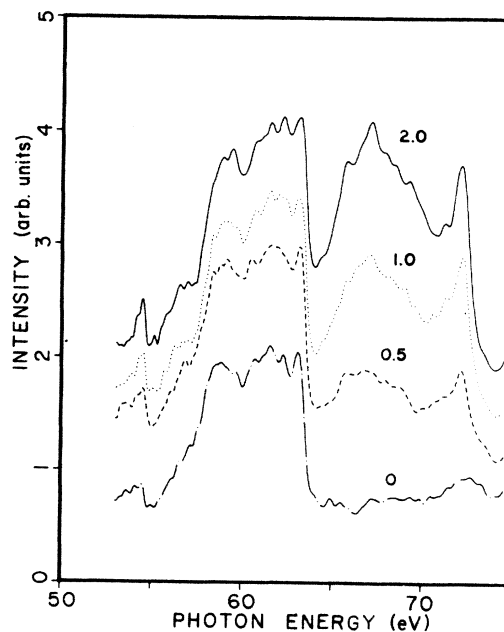


FIG. 2. The Mg L satellite and Al $L_{2,3}$ spectra for Mg metal and Al in Mg alloys. The spectra are labeled with the Al content in atomic percent.

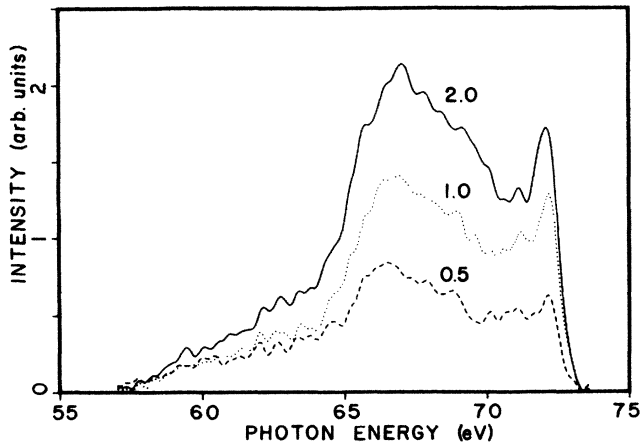


FIG. 3. The Al $L_{2,3}$ impurity spectra for Al in Mg alloys after subtraction of the Mg satellite spectrum. The spectra are labeled with Al content in atomic percent.

content, in excess of that obtained with pure Mg, is also observed that may be attributed to the Al component of the alloy.

Since both the Mg satellite and the Al spectrum lie in the Mg $L_{2,3}$ absorption band, the spectral intensity should be corrected for self-absorption by Mg. A simple one-dimensional model may be used for this correction in which the measured spectrum I is related to the internal spectrum I_0 by the expression

$$I(\lambda) = \int I_0(\lambda) \exp[-\mu(\lambda)x / \cos\theta_0] \\ \times F_{\text{exc}}(x / \cos\theta_i, E) dx,$$

where $F_{\text{exc}}(x / \cos\theta_i, E)$ is the probability of excitation of an atom at a depth x below the surface by an electron incident with energy E and angle θ_i , and $\mu(\lambda)$ is the absorption coefficient for x rays exiting at an angle θ_0 . The path lengths of the exciting electrons and exiting x rays at a depth x below the surface are denoted by $x / \cos\theta_i$ and $x / \cos\theta_0$. In the present case where the Mg satellite and Al spectra lie in a spectral region of strong Mg absorption, the escape depth for soft x rays, which may be calculated from the absorption coefficient for Mg,²⁸ is substantially smaller than the excitation depth for 2-kV incident electrons, which may be calculated from the stopping power of electrons in Mg and the inverse mean path for the excitation of $2p$ core holes.^{29,30} The excitation probability with depth is approximately constant until the incident electron's energy is reduced to a few hundred eV at a depth of about 900 Å. Under these conditions, which do not apply to the primary Mg spectrum, for which the absorption is small, the internal spectrum may be determined from the measured spectrum using the simple relation $I_0(\lambda) = \mu I(\lambda)$. This correction has been made to the impurity spectra in Fig. 3 using absorption coefficient μ for Mg taken from the literature.²⁸

RESULTS AND DISCUSSION

The $L_{2,3}$ spectrum of a 1-at. % alloy is shown in Fig. 1. The primary and satellite Mg spectra of the other

samples studied (pure Mg, and 0.5-at. % and 2-at. % alloys) are not measurably different from those shown here. The primary Mg spectrum has been discussed by several earlier authors.³¹ The threshold peak is a mixture of band-structure effects and the threshold anomaly of the MND many-body theory characterized by a threshold exponent α .^{20,21,32} The lower peak in the primary spectrum centered at 47.5 eV is a feature of the s PDOS of Mg. Below 45 eV, the intensity of the primary spectrum decreases rapidly, consistent with the theoretical bandwidth of 7.1 eV for Mg.³²

The spectra of the Mg satellite for pure Mg and for the alloy samples are shown in Fig. 2. The edge threshold is located at 63.5 ± 0.1 eV and lies 14.0 ± 0.1 eV above the parent band edge at 49.5 eV. This may be compared with the previous separation of 13.6 eV cited by Hanson and Arakawa using lower-resolution data.³³ The apparent small differences in shape for the satellite spectra as a function of Al impurity content are believed to be due to the tails of the Al spectra which extend below the satellites. These tails are clearly seen in Fig. 3 after the satellite spectrum is subtracted.

Three major peaks are resolved in the satellite spectrum: a threshold peak at 63.2 eV; a broad central peak at 61.6 eV; and a low-energy peak at 58.8 eV. Some of the smaller features in the spectra seem to be reproduced, but we believe that they result from noise and/or small calibration errors rather than from real features of the density of states. The central peak in the satellite spectrum was not resolved in earlier studies.³³

In Fig. 4, the satellite and primary peaks are compared by aligning their thresholds. The spectra were shifted by 13.99 eV to bring their edges into coincidence. Clearly the threshold peak and central peak of the satellite coincide with the threshold peak and secondary maximum visible in the parent spectrum. The low-energy peak of the satellite has no counterpart in the parent spectrum and is a structure that can be unambiguously identified with the presence of a hole in the final state of the system. We interpret this to be simply the screening enhancement expected for an additional core

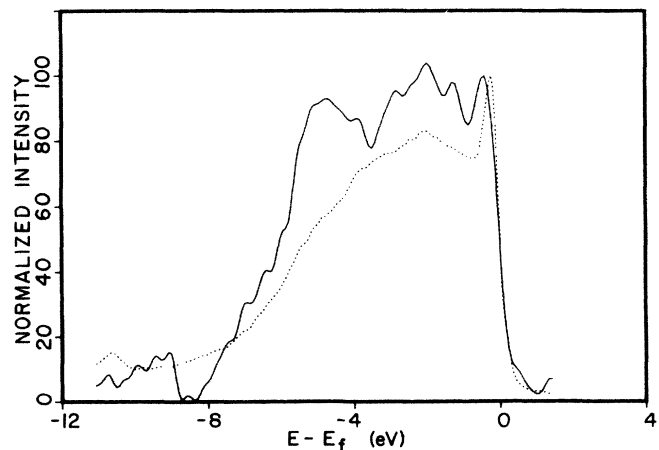


FIG. 4. The Mg satellite spectrum compared with the primary Mg $L_{2,3}$ spectrum. \cdots , primary spectrum; — , satellite spectrum.

hole.

It is also clear from Fig. 4 that the threshold peak of the satellite spectrum is not as sharp as that of the primary spectrum. This may constitute support for the calculations of von Barth and Grossman which suggest that the exponent for the MND threshold anomaly should be smaller in the satellite than in the primary spectrum.² The determination of the threshold anomaly exponent is difficult because of the presence of the band-structure peak at the threshold. Neddermeyer, from data virtually identical to ours, determined a value for the primary peak of $\alpha=0.3\pm 0.07$.³¹ We estimate the threshold anomaly exponent for the satellite to be $\alpha=0.16\pm 0.08$, assuming a similar contribution of the DOS to both the primary and satellite spectra.

In Fig. 2, a very weak spectral feature extends from about 67 to 74 eV in the pure Mg sample. Its intensity is about 10% of that of the main Mg satellite. The satellite is believed to represent decay from a state with two holes in the core ($2p^2$). This configuration contains three LS -coupling configuration terms, $^3P_{2,1,0}$, 1D_2 , and 1S_0 . Even though quantum weighting arguments would suggest that the 1D_2 state is produced with $\frac{5}{9}$ the probability of the 3P states in the excitation process, this state is believed to decay nonradiatively to the 3P prior to radiative decay. Thus the main satellite is believed to result from the decay of the 3P state.³⁴ The weaker high-energy structure that we observe may result from the radiative decay of the previously unobserved 1S_0 state. Its energy separation from the 3P_2 satellite is consistent with calculations of the separation of these states in free ions,³⁵ and its relative magnitude is consistent with the relative degeneracies of the 3P and 1S states.

We report for the first time observation of the L_3 - L_1 intercore transition for the satellite spectrum at 54.5 ± 0.1 eV. A careful comparison of the shape of this peak to the L_1 - L_3 intercore transition of the primary spectrum at 39 eV shows some apparent differences in shape, but noise in the data makes further analysis impractical. There is a clear difference in the energy separation between the Fermi edge of the primary spectrum and its associated intercore transition (10.7 eV) from the energy separation of the Fermi edge of the satellite and its intercore transition (9.0 eV). This difference may be of value for testing calculations of chemical shifts of electronic core states in alloys.

The impurity spectra for Al are shown in Fig. 3. The spectra increase linearly in intensity with the Al content, as do the sloping low-energy tails of the spectra and the scattering background. The scattering background has been subtracted in Fig. 3. As with the satellite spectrum, the small features in these spectra are thought to result from noise or calibration errors and probably do not represent real structure in the density of states.

In Fig. 5, the Al impurity spectrum is compared with the spectra of pure Al and Mg metals, with the spectra being aligned at their Fermi edges. It can be seen from Fig. 5 that the sloping tails of the alloy spectra extend to the full width of the pure Al spectrum. In addition to the processes producing tailing in all metal spectra, the effects of clustering may enhance the tails for

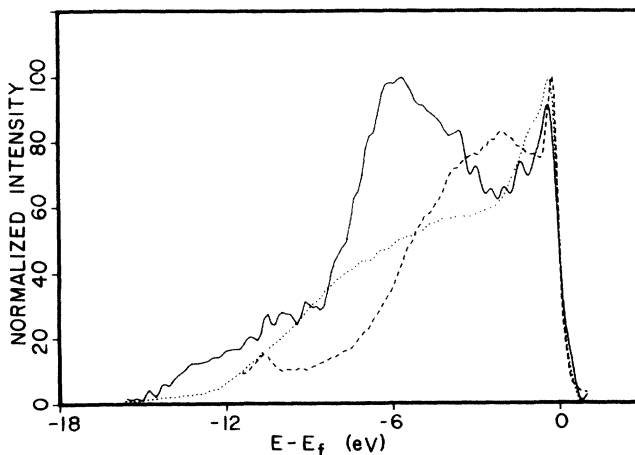


FIG. 5. The Al-impurity spectrum for the 1 at. % alloy compared with the $L_{2,3}$ spectra of pure Al and Mg. \cdots , Al metal; $-\ -$, Mg metal; $—$, Al impurity.

these alloy spectra. Except for the tails, a comparison of the spectra shown in Fig. 5 qualitatively confirms the idea that a $Z+1$ impurity in a free-electron metal will have a local DOS that is enhanced near the bottom of the band and that has a width equal to that of the host. Except for the tails, the Al impurity spectrum is enhanced at low energies and is narrowed toward the width of the Mg $L_{2,3}$ spectrum. The observed width is approximately 8.0 eV, but remains about 1 V wider than the primary Mg L spectrum.

We observe no change in the width of the Al spectra for the 0.5–2-at. % alloys (see Fig. 3). The failure to observe any change in spectral width with concentration suggests that the observed width is characteristic of the impurity limit, that the approximately 1 V difference in the widths of the Mg metal and Al impurity spectra is real, and that the source of the difference must be sought in the theoretical description of the SXE process.

The spectra may also be compared with the spectra obtained by Neddermeyer on richer alloys, who reports data on Al-Mg alloys with Al concentrations from 5 at. % to 67 at. %.⁴ The width observed for the 5-at. % alloy is probably comparable to that of our alloys, but a much more prominent low-energy tail is observed that presumably results from his somewhat poorer resolution and the failure to resolve and subtract the satellite spectrum. For richer alloys, the spectra clearly widen and approach the 12-eV width of the pure Al spectrum.

A threshold peak is visible in the Al-impurity spectra. In Fig. 6, the impurity spectrum in the threshold region is compared with the spectra of both pure Al and pure Mg. The Al spectra are plotted with the zero of the photon energy scale at 72.57 eV and the Mg spectrum has been shifted by 23.02 eV so that its high-energy edge is aligned with those of the Al alloy spectra. Both the edge width and threshold peak are slightly broader in the impurity spectrum than in the pure Al spectrum and much broader than in the Mg spectrum. The added width may be the result of added disorder near the Al site. The edge shape, though slightly broader, is clearly a better match to the Al than to the Mg edge. Since the

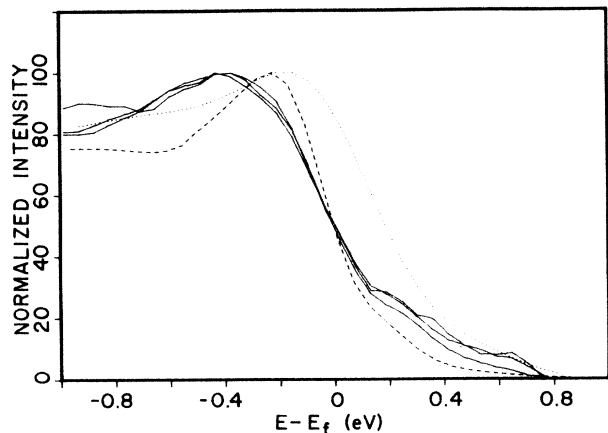


FIG. 6. The threshold region of the Al-impurity spectrum compared with pure Al and Mg. The zero of the energy scale is at 72.57 eV. The Mg spectrum has been shifted by 23.02 eV. \cdots , Al metal; $---$, Mg metal; $—$, Al impurity.

threshold peaks are believed to be associated with the MND many-body threshold anomaly, this is an important result that must be accounted for by theory.

Figure 6 also shows a 0.18-eV shift of the Fermi edge of the alloy spectrum from pure Al. This shift may be attributed to a "chemical" shift of the core level due to the change of the charge environment at the Al ion core.

In Fig. 7, the Al-impurity spectrum, the Mg satellite spectrum, and the Mg KL_1V Auger spectrum from Lasser and Fuggle⁵ are compared. Each of these spectra is believed to be derived primarily from the s PDOS of an ion core in Mg with an excess positive charge in the final state. Within the equivalent-core approximation, they would each be expected to have the same shape. Each is observed to have a prominent low-energy peak associated with the screening charge. The physical origin of these screening peaks has been properly identified by many earlier workers.^{2,5,6,9-15} Otherwise, the spectra show substantial differences. The Al-impurity spectrum

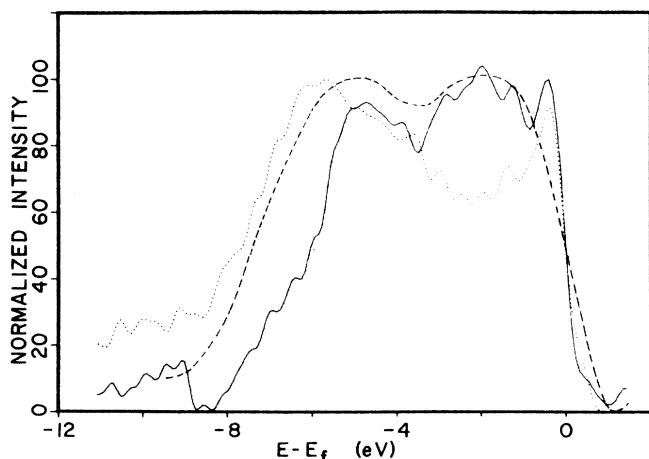


FIG. 7. The Mg L satellite, the 1 at. % Al $L_{2,3}$, and the KL_1V Auger spectra compared. \cdots , Al impurity; $---$, KL_1V Auger; $—$, Mg satellite. The Auger spectrum was taken from Ref. 5.

and the Auger spectrum are about 1 eV wider than the satellite spectrum, though in the case of the Auger spectrum this may be partly due to lower resolution in the measurement. The central peak in the Mg satellite spectrum coincides with structure in the Auger spectrum, but has no counterpart in the Al-impurity spectrum. We have previously shown in Fig. 4 that it corresponds to a band-structure feature in Mg.

Clearly, a more sophisticated approach than the ECA is required for the interpretation of SXE and other core-level spectra. On theoretical grounds, this conclusion is perhaps not unexpected, since a probable physical origin for the differences may be readily identified. The s -like valence orbitals penetrate inside the core-level sphere, and thus are subject to different potentials for the Al impurity and for Mg atoms with an extra $2p$ core hole. The ECA has been, however, an attractive qualitative idea that has frequently been used in the interpretation of various core-level spectra.^{2,5,6} The present results suggest that it is not a useful approximation in the present case.

We will summarize here the major conclusions of this paper. Several of these results are new and others confirm previous results as noted in the preceding text.

(1) The Mg L satellite spectrum and the $L_{2,3}$ spectrum of dilute Al in Mg have been observed with unprecedented resolution.

(2) The width of the Al-impurity spectrum is about 1 V wider than that of the Mg $L_{2,3}$ spectrum of the host. The excess width is independent of the Al concentration and thus is believed to be characteristic of the true impurity spectrum.

(3) Both the Mg satellite and Al-impurity spectra exhibit a low-energy peak in the s PDOS that is associated with the screening of an extra charge in the ion core.

(4) Except for the low-energy "screening" peak, the spectra of the Mg satellite and of dilute Al in Mg show dissimilar structures associated with local densities of states specific to each. Hence the ECA does not give an adequate description of the data.

(5) The threshold peak in the Al-impurity spectrum resembles that of the pure Al spectrum rather than that of the Mg host, though both the edge and peak show some additional broadening. Other features of the Mg L spectrum are also not observed in the Al-impurity spectrum.

(6) The threshold peak in the Mg satellite spectrum is not as sharp as in the primary Mg spectrum, a result of possible interest to MND theory.

(7) A "chemical" shift of the core levels can be seen in the displacement of the Al Fermi threshold by 0.18 eV from pure Al to dilute Al in Mg.

(8) The L_1-L_3 intercore transition associated with doubly ionized Mg $2p$ levels has been observed for the first time. Its 9.0-eV separation from the Fermi edge of the Mg satellite spectrum is observed to be substantially smaller than the 10.7-eV separation observed for the primary Mg spectrum.

(9) A very weak, second satellite peak has been observed that may result from radiative transitions from a 1S_0 state of the doubly ionized core.

ACKNOWLEDGMENTS

The authors are grateful to Mr. F. Biancanello of the NBS Metallurgy Division for preparing the samples used in this research. The research was supported by National Science Foundation Grant No. DMR-8503541, by the Science Alliance Center of Excellence Grant from the

state of Tennessee, and by the U.S. Department of Energy under Contract No. DE-AC05-84OR21400 with Martin Marietta Energy Systems. The research was carried out in part at the National Synchrotron Light Source at Brookhaven National Laboratory, which is supported by the U.S. Department of Energy under Contract No. DE-AC02-76CH00016.

*Also at Oak Ridge National Laboratory.

- ¹R. G. Oswald and T. A. Callcott, *Phys. Rev. B* **12**, 4122 (1971).
- ²U. von Barth and G. Grossman, *Phys. Scr.* **28**, 107 (1983).
- ³R. S. Crisp and S. E. Williams, *Philos. Mag.* **5**, 1205 (1960).
- ⁴H. Neddermeyer, in *Band Structure Spectroscopy of Metals and Alloys*, edited by D. J. Fabian and L. M. Watson (Academic, London, 1973), p. 153.
- ⁵R. Lasser and J. C. Fuggle, *Phys. Rev. B* **22**, 2637 (1980).
- ⁶P. H. Hannah, P. Weightman, and P. T. Andrews, *Phys. Rev. B* **31**, 6238 (1985); M. Davies and P. Weightman, *ibid.* **30**, 4183 (1980).
- ⁷B. L. Gyorffy and G. M. Stocks, in *Electrons in Disordered Metals and on Metallic Surfaces*, edited by P. Phariseau, B. J. Gyorffy, and L. Sheire (Plenum, New York, 1979), pp. 89–192.
- ⁸A. Bansil, L. Schwartz, and H. Ehrenreich, *Phys. Rev. B* **12**, 2893 (1975); **9**, 449 (1974).
- ⁹G. M. Stocks, J. A. Tagle, T. A. Callcott, and E. T. Arakawa, in *Inner-Shell X-Ray Physics of Atoms and Solids*, Proceedings of the International Conference on X-Ray Processes and Inner-Shell Ionization, England, 1980, edited by D. J. Fabian, H. Kleinpopper, and L. Watson (Plenum, New York, 1981), pp. 619–624.
- ¹⁰C. Koenig, N. Stefanou, and J. M. Koch, *Phys. Rev. B* **33**, 5307 (1986).
- ¹¹J. E. Inglesfield, *J. Phys. F* **2**, 878 (1972); **9**, 1551 (1979).
- ¹²J. C. Boisvert, P. W. Goalwin, A. B. Kunz, M. H. Bakshi, and C. P. Flynn, *Phys. Rev. B* **31**, 4984 (1985).
- ¹³M. A. Bull and Md. M. Islam, *J. Phys. F* **14**, 347 (1984).
- ¹⁴T. A. Callcott, J. A. Tagle, E. T. Arakawa, and G. M. Stocks, *Appl. Opt.* **19**, 4035 (1980); *Phys. Rev. B* **22**, 2716 (1980).
- ¹⁵R. S. Crisp, *J. Phys. F* **11**, 1705 (1981).
- ¹⁶G. D. Mahan, *Phys. Rev. B* **21**, 1421 (1980).
- ¹⁷U. von Barth and G. Grossman, *Solid State Commun.* **32**, 645 (1979).
- ¹⁸U. von Barth and G. Grossman, *Phys. Rev. B* **25**, 5150 (1980).
- ¹⁹L. C. Davis and L. A. Feldcamp, *Phys. Rev. B* **23**, 4269 (1981).
- ²⁰G. D. Mahan, *Phys. Rev.* **163**, 612 (1969).
- ²¹P. Nozières and C. T. de Dominicis, *Phys. Rev.* **178**, 1096 (1969).
- ²²M. O. Krause, *J. Phys. Chem. Ref. Data* **8**, 307 (1979).
- ²³T. A. Callcott, K.-L. Tsang, C. H. Zhang, D. L. Ederer, and E. T. Arakawa, *Rev. Sci. Instrum.* **57**, 2680 (1986).
- ²⁴H. S. Gotts and A. J. Glick, *Phys. Rev. B* **23**, 4337 (1981).
- ²⁵G. A. Rooke, *Phys. Lett.* **3**, 234 (1963).
- ²⁶P. Longe and A. J. Glick, *Phys. Rev.* **177**, 526 (1969).
- ²⁷J. A. R. Samson, *Techniques of Vacuum Ultraviolet Spectroscopy* (Wiley, New York, 1967), p. 10.
- ²⁸H. J. Hagemann, W. Gudat, and C. Kunz, *J. Opt. Soc. Am.* **65**, 742 (1975).
- ²⁹J. C. Ashley, C. J. Tung, and R. H. Ritchie, *Surf. Sci.* **81**, 409 (1979). Methods of calculation are illustrated in this reference for Al.
- ³⁰Calculations for Mg may be made from data in E. J. McGuire, *Phys. Rev. A* **16**, 73 (1977), and C. J. Powell, *Surf. Interface Anal.* **7**, 263 (1985).
- ³¹H. Neddermeyer, *Phys. Rev. B* **13**, 263 (1976).
- ³²R. P. Gupta and A. J. Freeman, *Phys. Rev. Lett.* **36**, 1194 (1976).
- ³³W. F. Hanson and E. T. Arakawa, *Z. Phys.* **251**, 271 (1972).
- ³⁴C. O. Almbladh and U. von Barth, *J. Phys. C* **8**, 4117 (1975).
- ³⁵E. H. Kennard and E. Ramberg, *Phys. Rev.* **46**, 1040 (1934).